Appendix D Hypocenter Location Distribution

D.1.1 RESULTS

Chiou and Youngs [2008; see Appendix B] developed the distribution for along-strike location of the hypocenter shown in Figure D.1. The figure shows an empirical distribution for the normalized along-strike hypocenter location $X = L_H/L_R$, where L_H is the distance of the hypocenter from one end of the rupture, and L_R is the rupture length. The distribution was developed using the finite-fault rupture model database compiled by Mai et al. [2005]. As the focus of the analysis presented in Appendix B of Chiou and Youngs [2008] was on the evaluation of distance metrics for moderate-magnitude earthquakes, they used only the data from Mai et al. [2005] for $\mathbf{M} \leq 6.5$ earthquakes. They also found no significant effect of style of faulting on the distribution for X within the dataset for moderate-magnitude earthquakes.

The distribution for X developed by Chiou and Youngs (2008] indicated a preference for bi-lateral ruptures. More recently, McGuire et al. [2002] reported that large earthquakes show a tendency for unilateral ruptures. They based their evaluation on assessing the second moment of the space-time moment release functions of large earthquakes, which considered all types of shallow earthquakes (crustal and subduction zone) and did not examine the effect of style of faulting. Their method also did not distinguish between along strike and down-dip hypocenter locations.

Dr. Mai and his colleagues have greatly expanded the rupture model database of Mai et al. [2005]. The updated database (http://equake-rc.info/SRCMOD, accessed April 24, 2014) was accessed to extract hypocenter location data for shallow crustal earthquakes of $\mathbf{M} > 6.5$. The resulting values are listed in Table D.1. Figure D.2 compares the empirical distribution for X for the earthquakes listed in Table D.2, separated into strike-slip and reverse categories, to the distribution for $\mathbf{M} \leq 6.5$ earthquakes of all slip types developed by Chiou and Youngs [2008]. Because the selection of which end of the rupture to use to define L_H for forward applications is arbitrary, the values of X have been folded into half ruptures (e.g., $X = 0.1$ is equivalent to $X = 0.9$). The distribution of X for large-magnitude reverse-faulting earthquakes is similar to that developed for moderate-magnitude earthquakes of all faulting styles, indicating a preference for bilateral along-strike ruptures; however, the data for large-magnitude strike–slip earthquakes shows a bimodal distribution for X, with approximately half of the ruptures being bilateral and the other half being nearly unilateral.

Figure D.3 shows the distributions for an along-strike hypocentral location ratio X recommended for use in modeling directivity effects for large-magnitude earthquakes. The recommended distribution for reverse faulting is the same as the model distribution shown in

Figure D.1 because the data for large-magnitude reverse earthquakes have a similar distribution to that for the moderate-magnitude earthquakes. The recommended distribution for strike–slip earthquakes is bimodal, with half of the rupture being nearly unilateral (X in the range of 0 to 0.2) and half being nearly bilateral (X in the range of 0.3 to 0.7).

D.1.2 REFERENCES

Chiou B.C.-J., Youngs R.R. [2008]. NGA model for average horizontal component of peak ground motion and response spectra, PEER Report No. 2008/09, Pacific Earthquake Engineering Research Center, University of California, Berkeley, CA.

Mai P.M., Spudich P., Boatwright J. (2005). Hypocenter locations in finite-source rupture models, *Bull. Seismol. Soc. Am.*, 95: 965–980.

McGuire J.J., Zhao L., Jordan T.H. [2002]. Predominance of unilateral rupture for a global catalog of large earthquakes, *Bull. Seismol. Soc. Am.*, 92: 3309–3317.

Table D.1 Along strike hypocenter location data for shallow crustal earthquakes extracted from http://equake-rc.info/SRCMOD (accessed April 24, 2014).

Earthquake	Date	Latitude	Longitude	M	Style of Faulting	*X*
San Fernando (Calif.)	2/9/1971	34.43	-118.37	6.82	Rev	0.36
Tabas (Iran)	9/16/1978	33.22	57.36	7.09	Rev	0.21
Imperial Valley (Calif.)	10/15/1979	32.644	-115.3	6.53	SS	0.00
Borah Peak (Idaho)	10/28/1983	44.06	-113.86	6.82	Rev	0.15
Nahanni1 (Canada)	10/5/1985	62.208	-124.21	6.66	Rev	0.30
Nahanni2 (Canada)	12/23/1985	62.187	-124.24	6.66	Rev	0.47
Superstition Hills (Calif.)	11/24/1987	33.016	-115.85	6.60	SS	0.08
Elmore Ranch (Calif.)	11/24/1987	33.083	-115.79	6.52	SS	0.20
Loma Prieta (Calif.)	10/18/1989	37.041	-121.88	6.91	Rev	0.43
Landers (Calif.)	6/28/1992	34.2	-116.43	7.20	SS	0.14
Northridge (Calif.)	1/17/1994	34.213	-118.53	6.80	Rev	0.17
Kobe (Japan)	1/17/1995	34.598	135.044	7.02	SS	0.32
Zirkuh (East Iran)	5/10/1997	33.82	59.8	7.22	SS	0.03
Izmit (Turkey)	8/17/1999	40.7	29.91	7.47	SS	0.40
ChiChi (Taiwan)	9/20/1999	23.869	120.84	7.63	Rev	0.35
Hector Mine (Calif.)	10/16/1999	34.59	-116.27	7.14	SS	0.39
Duzce (Turkey)	11/12/1999	40.818	31.198	7.18	SS	0.46
Tottori (Japan)	10/6/2000	35.275	133.35	6.79	Rev	0.50
Bhuj,India	1/26/2001	23.403	70.2835	7.60	Rev	0.38
Denali (Alaska)	11/3/2002	61.514	-147.45	7.87	SS	0.08
Boumerdes (Algeria)	5/21/2003	36.83	3.65	7.25	Rev	0.41
Bam, Iran	12/26/2003	29.052	58.365	6.54	SS	0.50
Irian-Jaya, Indonesia	2/7/2004	-3.99	135.051	7.20	SS	0.38
Fukuoka (Japan)	3/20/2005	33.75	130.16	6.67	SS	0.42
Kashmir	10/8/2005	34.49	73.6253	7.60	Rev	0.39
Niigata-ken Chuetsu-oki	8/17/2007	37.54	138.61	6.77	Rev	0.26
Wenchuan, China	5/12/2008	30.986	103.364	8.07	Rev	0.11
Iwate - Miyagi Nairiku	6/13/2008	39.027	140.878	7.01	Rev	0.50
Honshu, Japan	6/13/2008	39.109	140.677	6.80	Rev	0.46
Gulf of California	8/3/2009	29.409	-112.8	6.90	SS	0.47
Haiti	1/12/2010	18.5	-72.53	7.00	Rev	0.23
El Mayor-Cucapah, Mexico	4/4/2010	32.3	-115.26	7.33	Rev	0.10
Darfield, New Zealand	9/3/2010	-43.55	172.2	7.10	Rev	0.06
Pakistan	1/18/2011	28.842	63.9578	7.20	Rev	0.46
Van, Turkey	10/23/2011	38.628	43.486	7.13	Rev	0.39
Masset, Canada	10/28/2012	52.769	-131.92	7.72	Rev	0.46
Khash, Iran	4/16/2013	28.113	62.048	7.80	Rev	0.50
Balochistan, Pakistan	9/24/2013	26.87	65.325	7.70	SS	0.14

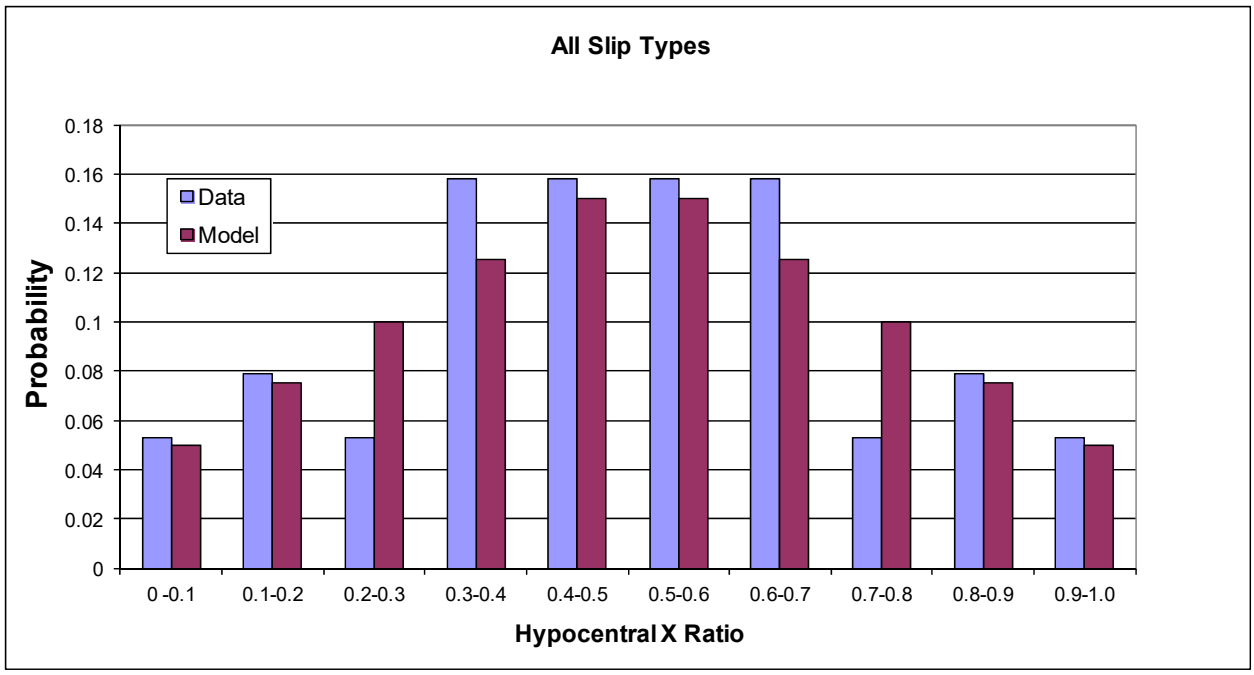

Figure D.1 **Distribution for along strike hypocenter location developed by Chiou and Youngs [2008].**

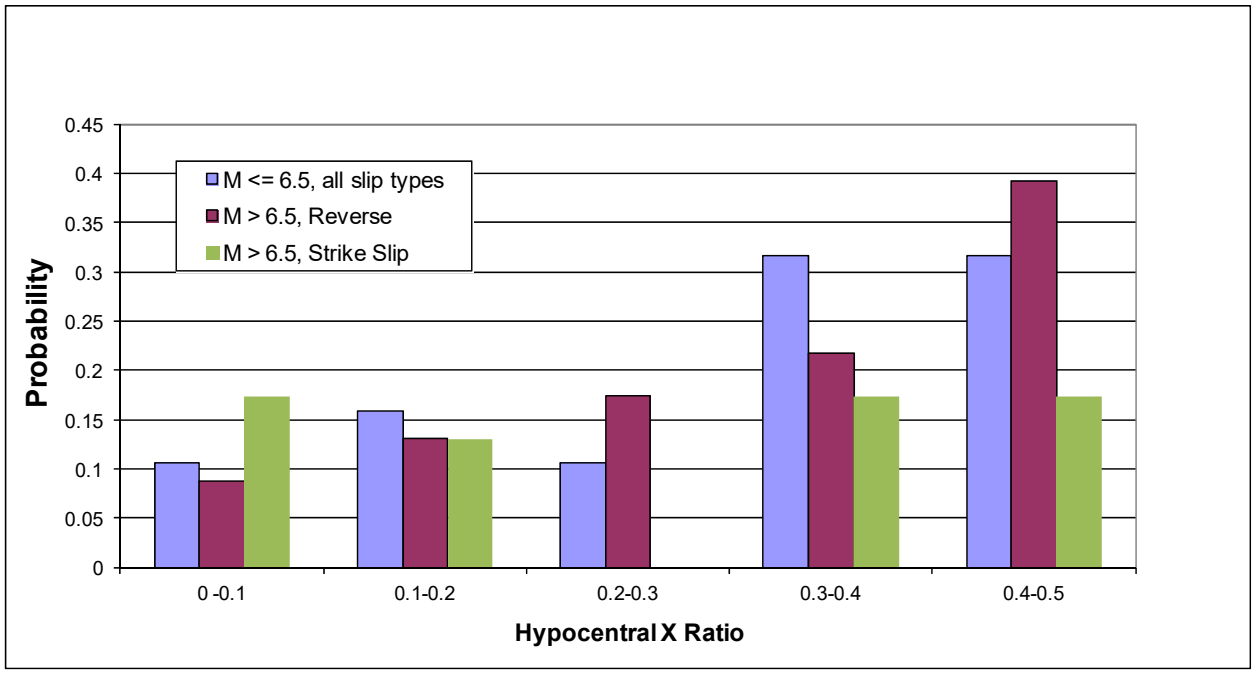

Figure D.2 **Comparison of distribution for along strike hypocenter location ratio X developed by Chiou and Youngs [2008] for M ≤ 6.5 with distributions for M > 6.5 earthquakes.**

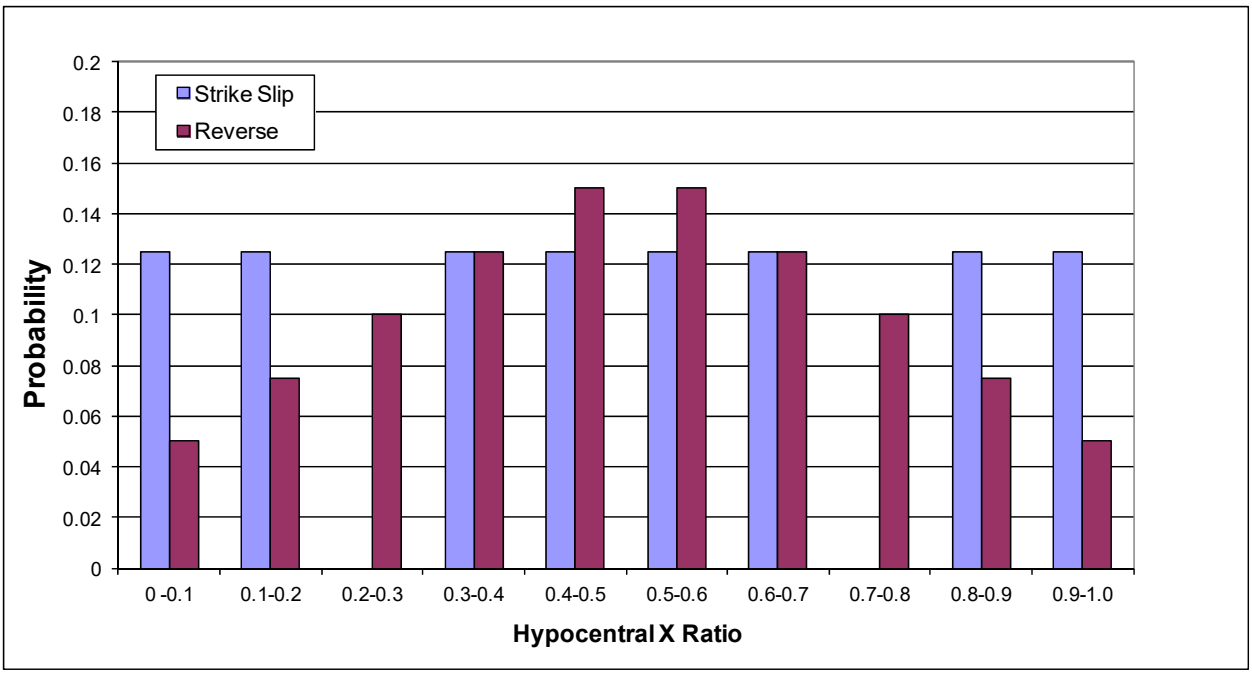

Figure D.3 Recommend distributions for along strike hypocenter location ratio *X*.